

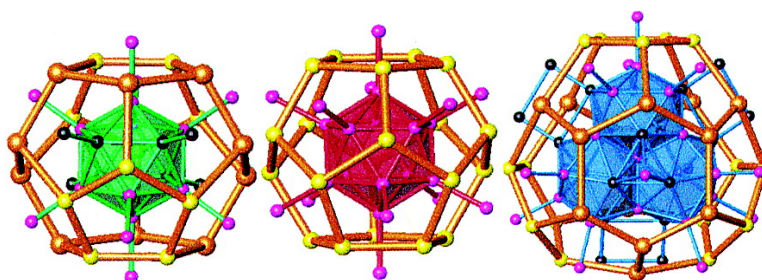
Article

Phase Stabilization through Electronic Tuning: Electron-Poorer Alkali-Metal–Indium Compounds with Unprecedented In/Li Clusters

Bin Li, and John D. Corbett

J. Am. Chem. Soc., **2005**, 127 (3), 926-932 • DOI: 10.1021/ja0402046 • Publication Date (Web): 30 December 2004

Downloaded from <http://pubs.acs.org> on March 24, 2009



More About This Article

Additional resources and features associated with this article are available within the HTML version:

- Supporting Information
- Links to the 9 articles that cite this article, as of the time of this article download
- Access to high resolution figures
- Links to articles and content related to this article
- Copyright permission to reproduce figures and/or text from this article

[View the Full Text HTML](#)



Phase Stabilization through Electronic Tuning: Electron-Poorer Alkali-Metal–Indium Compounds with Unprecedented In/Li Clusters

Bin Li and John D. Corbett*

Contribution from the Ames Laboratory-DOE¹ and Department of Chemistry,
Iowa State University, Ames, Iowa 50011

Received August 27, 2004; E-mail: jcorbett@iastate.edu

Abstract: Three alkali-metal–indium compounds $K_{34}In_{92.30}Li_{12.70}$ (I), $K_{14}Na_{20}In_{91.82}Li_{13.18}$ (II), and $K_{14}Na_{20}In_{96.30}$ (III) (all $R\bar{3}m$) have been synthesized and characterized by structural and physical property measurements and electronic structure calculations. Novel mixed In/Li anionic icosahedra and fused icosahedra form in I and II. All three contain In_{28} as the first triply fused In icosahedra, which are further linked into $(In_{28})_n(In_{28})$ sandwich adducts in compounds I and II and $(In_{28})_2(In_{28})$ in III. Stabilization of these electron-poorer phases through electronic tuning occurs via two different structural (redox) perturbations, either by substitution of certain indium atoms in the clusters by electron-poorer lithium atoms or by the introduction of defects and disorder in the fused cluster (III). The preferential occurrence of either substitutions or defect formation in the clusters is consistent with extended Hückel band calculation results for both the ideal pure indium phase and the Li-substituted equivalent. Model (ideal) and experimental E_F values (based on stoichiometries) fall around a pseudogap in DOS. All three compounds are metallic according to both EHTB band calculations and measured resistivities. The cations ($A = K, Na$) in all the three structures generate A_{136} clathrate-II type networks with remarkably specific and transferable cation dispositions around the two types of anionic cluster units.

Introduction

Exploratory synthetic efforts within the alkali-metal–trial systems, particularly within the Ga, In, and Tl family, have revealed many examples with remarkable structural diversities and novel chemical bonding. Gallium and indium generally form extended anionic cluster frameworks, with only a few examples of discrete clusters, principally for indium, whereas thallium chemistry is rich in isolated cluster moieties reminiscent of borane chemistry.^{2,3} Icosahedral or icosahedral-based clusters are very common for these triels.⁴ Removal of one or two icosahedral vertexes may produce *nido* or *arachno* derivatives, respectively, as in $Na_{15}In_{27.4}$.⁵ Application of the Zintl–Klemm electron counting scheme and Wade’s cluster bonding descriptions show that the cluster phases essentially exhibit closed-shell counts, indicating a common drive to achieve these configurations according to electronic rules even though many are still poor metals. Compensation for electron deficiencies in the structures also can occur through condensation of icosahedral building blocks, such as by vertex-, edge-, or face-sharing. Such complex examples have been reported mainly for gallium,

twinned gallium icosahedra in $Li_9K_3Ga_{28.83}$ ⁶ and $Li_3Na_5Ga_{19.57}$,⁷ and triply fused icosahedra in $Na_{13}K_4Ga_{47.45}$ ⁸ and $Na_{102}(MGa)_{315}$ ($M = Zn, Cu$).⁹ However, neither of these modes has been reported to date among indium or thallium cluster compounds.

A considerable number of novel indium and thallium clusters that are not known in binary systems can also be isolated via the size tuning with mixed cations to achieve better packing in the lattices.^{2,4} Examples include KNa_3In_9 ,¹⁰ $Na_2K_{19}Tl_{21}$,¹¹ $Na_{14}K_6Tl_{18}Mg$,¹² and $Na_4K_6Tl_{13}$,¹³ and a remarkable indium network in K_2SrIn_7 in which cation charge also varies.¹⁴ Despite the large number of new compounds so discovered, synthetic investigations have so far not included lithium in ternary alkali-metal–indium or –thallium systems.

Continuing research on these has now led to the discovery of the three unusual compounds with the first triply fused indium icosahedra as In_{28} . It also turns out that doping one compound that shows defects and disorder in the indium networks with lithium gives defect-free and ordered structures, a remarkable example of phase stabilization through electronic tuning.

(1) This research was supported by the Office of the Basic Energy Sciences, Materials Sciences Division, U.S. Department of Energy (DOE). The Ames Laboratory is operated for DOE by Iowa State University under Contract No. W-7405-Eng-82.
(2) Belin, C. H. E.; Charbonnel, M. *Prog. Solid State Chem.* **1993**, *22*, 59.
(3) Corbett, J. D. In *Chemistry, Structure and Bonding of Zintl Phases and Ions*; Kauzlarich, S., Ed.; VCH Publishers: New York, 1996; Chapter 3.
(4) Corbett, J. D. *Angew. Chem., Int. Ed.* **2000**, *39*, 670.
(5) Sevov, S. C.; Corbett, J. D. *J. Solid State Chem.* **1993**, *103*, 114.

(6) Belin, C. H. E. *J. Solid State Chem.* **1983**, *50*, 225.
(7) Charbonnel, M.; Belin, C. H. E. *Nouv. J. Chim.* **1984**, *10*, 595.
(8) Belin, C. H. E.; Charbonnel, M. *J. Solid State Chem.* **1986**, *64*, 57.
(9) Charbonnel, M.; Chouaibi, N.; Belin, C. *J. Solid State Chem.* **1992**, *100*, 220. Charbonnel, M.; Chouaibi, N.; Belin, C. *C. R. Acad. Sci. Paris* **1992**, *315*, 661.
(10) Li, B.; Corbett, J. D. *Inorg. Chem.* **2002**, *41*, 3944.
(11) Dong, Z.-C.; Corbett, J. D. *J. Am. Chem. Soc.* **1994**, *116*, 3429.
(12) Dong, Z.-C.; Corbett, J. D. *Angew. Chem., Int. Ed. Engl.* **1996**, *35*, 1006.
(13) Dong, Z.-C.; Corbett, J. D. *J. Am. Chem. Soc.* **1995**, *117*, 6447.
(14) Chi, L.; Corbett, J. D. *Inorg. Chem.* **2001**, *40*, 3596.

Experimental Section

Syntheses. All materials were handled in He- or Ar-filled gloveboxes that had moisture levels below 1 ppm (vol.). All three compounds were synthesized via high-temperature reactions of the pure elements (sodium chunks, 99.95%, potassium chunks, 99.95%, lithium ribbons, 99.9%, and indium tear drops, 99.99%, all from Alfa-Aesar). The weighed elements were enclosed in welded niobium tubes that were in turn sealed in evacuated fused silica jackets by methods and techniques described previously.¹⁵ A single crystal of $K_{14}Na_{20}In_{96.30(1)}$ (**III**) was first obtained from a NaKIn₅ loading. Even though several apparently very good single crystals were selected for data collection, no satisfactory refinement could be achieved. Later, lithium was added with the idea of substituting it for some of the Na or K cations to gain new packing and possibly new clusters, but two related substitution compounds were obtained instead. Solution of their structures revealed unexpected mixed In/Li clusters, namely $K_{34}In_{92.30}Li_{12.70}$ (**I**) and $K_{14}Na_{20}In_{91.82}Li_{13.18}$ (**II**), whereafter the structure of **III** was solved with the aid of that of **II** as a model. Once all stoichiometries had been established by crystallography, high purity phases of all three were obtained separately from stoichiometric syntheses, as judged by comparison of their Guinier powder patterns with those calculated for the refined structures. All three can be made by heating appropriate samples at 550 °C for ~5 h, cooling these at 10 °C/h to 250 °C, and holding them there for ~160 h to grow crystals. Phase **I** appears to be a line phase in that an attempt to synthesize it with more Li and fewer electrons (see the band calculation results) showed no change in the Guinier lattice constants. Also attempts to synthesize anything near an isostructural $K_{34}In_{105}$ binary phase (**I** without lithium) failed, giving instead $K_{22}In_{39}$ and KIn_4 . All products are silvery, brittle, and very sensitive to moisture and air.

X-ray Studies. X-ray diffraction investigations were performed on powdered samples and single crystals. Powder data were collected with the aid of a Huber 670 Guinier powder camera equipped with an area detector and Cu K α radiation ($\lambda = 1.540598 \text{ \AA}$). Powdered samples were homogeneously dispersed between two layers of Mylar with the aid of a little vacuum grease. The step size was set at 0.005° , and the exposure time was 0.5 h. Data acquisition was controlled via the in situ program. Peak search, indexing, and least-squares refinements for cell parameters were done with the Rietica program.¹⁶ Single-crystal X-ray diffraction techniques were used for detailed structural analyses. Diffraction data were collected at 293 K with the aid of a Bruker SMART APEX CCD diffractometer and Mo K α radiation, these being harvested from three sets of 606 frames obtained with 0.3° scans in ω and exposure times of 10 s per frame over a 2θ range of $\sim 3^\circ$ to $\sim 57^\circ$. The unit cell parameters were determined from data for about 900 indexed reflections. The reflection intensities were integrated with the SAINT subprogram in the SMART software package.¹⁷ The data were corrected for Lorentz and polarization effects, and the program SADABS¹⁸ was applied for empirical absorption corrections. The structure solution was obtained by direct methods and refined by full-matrix least-squares refinements of F_o^2 using the Bruker SHELXTL 6.1 software package.¹⁹ Table 1 lists some crystallographic data for the three compounds, and Table 2 gives the corresponding atomic coordinates and occupancy data. More detailed crystallographic and refinement data and the anisotropic displacement parameters are available in the Supporting Information.

The observed extinction conditions and the intensity statistics for all three data sets were consistent with the $R\bar{3}m$ space group, and this gave satisfactory refinement results for all three compounds. For **I**, direct methods provided 15 peaks with distances among them that were appropriate for indium atoms, and they were so assigned. A few least-squares cycles followed by a difference Fourier map revealed six less

Table 1. Some Single Crystal and Structure Refinement Data for $K_{34}In_{92.30}Li_{12.70}$ (**I**), $K_{14}Na_{20}In_{91.82}Li_{13.18}$ (**II**), and $K_{14}Na_{20}In_{96.30}$ (**III**)

composition	I $K_{34}In_{92.298(7)}Li_{12.702(7)}$	II $K_{14}Na_{20}In_{91.818(8)}Li_{13.182(8)}$	III $K_{14}Na_{20}In_{96.30(1)}$
space group, Z	$R\bar{3}m$ (No. 166), 3		
a (\AA) ^a	18.6452(5)	18.2096(3)	18.0885(6)
c (\AA)	40.168(2)	39.527(2)	39.432(2)
V (\AA^3)	12093.2(8)	11350.7(5)	11173.4(8)
d_{cal} (g/cm^3)	4.949	5.109	5.383
abs. coeff (mm^{-1})	13.77	14.11	15.03
$R1/wR2$ [$I > 2\sigma(I)$]	0.0245/0.0470	0.0258/0.0544	0.0350/0.0862
residual peak/hole ($e/\text{\AA}^3$)	1.43, -2.12	1.52, -3.54	5.24, -2.84

^a Refined from Guinier powder data, $\lambda = 1.540562 \text{ \AA}$, 23 °C.

strongly diffracting atoms with distances appropriate to potassium atoms, and they were so assigned. But it became clear after a few more cycles that indium alone was too heavy for the 4 of the 15 indium positions: In2, In4, In12, and In13. (The atom numbering scheme is illustrated in the Supporting Information.) At this point R1 and the highest difference peak were 0.101 and $9.33 e/\text{\AA}^3$, respectively. Allowing lithium to admix at the four indium positions with varying isotropic displacement parameters gave significant improvements in R1 (0.055) and a highest difference peak of $5.93 e/\text{\AA}^3$ that was close to In15. Refinement, finally with anisotropic displacement parameters for all atoms, converged at $R1 = 0.0245$ and $wR2 = 0.0470$. The largest residual peak was $1.43 e/\text{\AA}^3$, 1.23 \AA from In15.

Even though lithium is significantly different from its heavier homologues in physical and chemical properties,²⁰ it is still surprising that lithium mixes with indium on the same atom positions. However, the refinement is consistent with the accurate lithium compositions determined by chemical analyses (atomic absorption). The failure to synthesize the isostructural binary K–In compound or any comparable phase without Li also indirectly indicates that lithium is necessary for the anionic structure with only K cations. The successful synthesis and structural refinement of compound **II** with 20 of 34 K atoms replaced by ordered Na atoms further confirmed that the same indium positions were co-occupied with somewhat different amounts of Li, as shown in Table 2, and consisted with chemical analyses.

For compound **III**, $K_{14}Na_{20}In_{96.30(1)}$, direct methods in the $R\bar{3}m$ space group provided 13 peaks with distances to each other that were appropriate for indium, and they were so assigned. A few least-squares cycles followed by a difference Fourier map revealed six less strongly diffracting atoms with distances appropriate for potassium and sodium atoms, and they were so assigned on the basis of peak heights. It became clear after a few more cycles that pure indium was too heavy for three of the indium positions: In12, In13, and In15. Moreover, R1 and the highest difference peak were then 0.131 and $38.7 e/\text{\AA}^3$ (0.87 \AA from In12), respectively. Relative to the **I** and **II** models, two more atoms positions (In11 and In14) also yielded large thermal parameters when assigned as In. When the occupancies of all five atoms were allowed to vary successively, three of the five gave partial occupancies but the last two did not show any significant decrease. Electron density maps of these five positions were unusual compared with those for crystals **I** and **II**. Three of them, In12, In13, and In15, had smaller electron densities, consistent with the partial occupancies of those positions, and they were so assigned for later refinement. Electron density maps of In11, In14, and In15 in compounds **II** and **III** are compared in the Supporting Information, Figure S1. Two, In11 and In14, were so shown to be split in **III**. The presence of a superstructure was not supported by additional Bragg reflections. Treating these two atoms as split gave significant improvements in R1 (0.068) and in the highest difference peak ($11.14 e/\text{\AA}^3$, close to In9) before final refinements of positional and anisotropic displacement parameters for all atoms ($R1 = 0.035$). Occupancy refinements for In1–In10 showed that all of these positions

(15) Dong, Z.-C.; Corbett, J. D. *J. Am. Chem. Soc.* **1993**, *115*, 11299.

(16) Hunter, B. A. *LHPM-Rietica Rietveld*, version 1.71; Australia, 1997.

(17) SMART; Bruker AXS, Inc.; Madison, WI, 1996.

(18) Blessing, R. H. *Acta Crystallogr.* **1995**, *A51*, 33.

(19) SHELXTL; Bruker AXS, Inc.; Madison, WI, 2000.

(20) Nesper, R. *Prog. Solid State Chem.* **1990**, *20*, 1.

Table 2. Atomic Positional Coordinates ($\times 10^4$), Isotropic Displacement Parameters, and Site Occupancies for $K_{34}In_{92.298(7)}Li_{12.702(7)}$ (I), $K_{14}Na_{20}In_{91.818(8)}Li_{13.182(8)}$ (II), and $K_{14}Na_{20}In_{96.30(1)}$ (III)^a

atom	x	y	z	U(eq)	Occ ^b
I					
In1	92(1)	3682(1)	363(1)	20(1)	0.647/0.353(2)
M2	1732(1)	5(1)	3213(1)	20(1)	
In3	393(1)	2525(1)	784(1)	21(1)	
M4	2498(1)	358(1)	1542(1)	22(1)	
In5	3879(1)	-x	1088(1)	15(1)	
In6	4459(1)	-x	489(1)	17(1)	
In7	5415(1)	-x	654(1)	20(1)	
In8	4210(1)	-x	1807(1)	14(1)	
In9	5701(1)	-x	1361(1)	20(1)	
In10	5126(1)	-x	1953(1)	17(1)	
In11	7549(1)	-x	2348(1)	19(1)	
M12	7205(1)	-x	1610(1)	18(1)	
M13	6093(1)	-x	2815(1)	26(1)	
In14	0	0	1130(1)	20(1)	
In15	0	0	0	40(1)	
K1	7954(1)	-x	929(1)	38(1)	
K2	0	0	2591(1)	40(1)	
K3	5345(1)	-x	3449(1)	36(1)	
K4	379(1)	4159(1)	1221(1)	19(1)	
K5	4455(1)	-x	2693(1)	20(1)	
K6	0	0	3614(1)	22(1)	
II					
In1	113(1)	3698(1)	367(1)	19(1)	0.687/0.313(2)
M2	1713(1)	24(1)	3224(1)	29(1)	
In3	411(1)	2578(1)	797(1)	19(1)	
M4	2526(1)	311(1)	1550(1)	22(1)	
In5	3881(1)	-x	1085(1)	22(1)	
In6	4430(1)	-x	506(1)	18(1)	
In7	5404(1)	-x	654(1)	19(1)	
In8	4208(1)	-x	1806(1)	17(1)	
In9	5674(1)	-x	1353(1)	17(1)	
In10	5088(1)	-x	1940(1)	20(1)	
In11	7563(1)	-x	2336(1)	17(1)	
M12	7219(1)	-x	1598(1)	17(1)	
M13	6086(1)	-x	2804(1)	20(1)	
In14	0	0	1142(1)	16(1)	
In15	0	0	0	31(1)	
K1	7954(1)	-x	924(1)	34(1)	
K2	0	0	2606(1)	32(1)	
K3	5336(1)	-x	3444(1)	30(1)	
Na1	417(2)	4194(2)	1218(1)	27(1)	
Na2	4442(1)	-x	2682(1)	20(1)	
Na3	0	0	3632(2)	18(1)	
III					
In1	120(1)	3671(1)	379(1)	21(1)	0.33(1)
In2	1727(1)	18(1)	3230(1)	21(1)	
In3	375(1)	2478(1)	794(1)	28(1)	
In4	2433(1)	342(1)	1546(1)	25(1)	
In5	3882(1)	-x	1090(1)	28(1)	
In6	4447(1)	-x	521(1)	24(1)	
In7	5409(1)	-x	683(1)	25(1)	
In8	4214(1)	-x	1801(1)	28(1)	
In9	5756(1)	-x	1372(1)	36(1)	
In10	5096(1)	-x	1941(1)	22(1)	
In11A	7523(2)	-x	2380(1)	30(2)	
In11B	7305(1)	-x	2280(1)	38(1)	
In12	7142(4)	-x	1565(2)	62(3)	
In13	6094(1)	-x	2901(1)	24(1)	
In14A	0	0	1692(1)	51(1)	
In14B	0	0	1207(2)	97(4)	
In15	0	0	339(3)	57(5)	
K1	7959(1)	-x	945(1)	36(1)	
K2	0	0	2627(1)	37(1)	
K3	5320(1)	-x	3446(1)	43(1)	
Na1	356(2)	4127(2)	1231(1)	30(1)	
Na2	4464(2)	-x	2663(1)	30(1)	
Na3	0	0	3655(2)	32(2)	

^a Hexagonal setting. ^b Occupancy for In/Li in compound I and II and for In atom in compound III.

are fully occupied, which is different from those for I and II wherein In2 and In4 sites were co-occupied by Li and In. The partial occupancies and the evident presence of split positions for In₁₁ and In₁₄ are responsible for the higher wR2 value and a residual of 5.14 e⁻/Å³ which is 0.82 Å from In14.

Attempts to find a better solution in lower symmetry space groups *R3m*, *R32*, *R3̄*, *R3*, *C/2m*, and even *P1* failed, these still showing partial occupancies and split peaks at the corresponding positions. Two additional crystals were picked from another reaction to obtain more precise atomic positions, but their structure refinements from CCD data gave similar map results. An additional X-ray diffraction data set was also collected at room temperature on a Rigaku AFC6R diffractometer for a crystal from a reaction with a different composition and carried out under different temperature conditions. However, refinement of these data gave a virtually identical result as that from CCD data.

Elemental Analyses. To confirm the lithium composition in the compound I and II, atomic absorption analysis was utilized. For that purpose, a few single crystals from each compound were carefully selected, weighed in the glovebox, and dissolved in dilute acid. Multiple measurements gave weight percentages of lithium of 0.66% and 0.73%, respectively, compared with those according to the refined formulae, 0.73(4)% and 0.79(5)%, respectively. Considering the accuracy of the sample weighing these numbers are in excellent agreement.

Physical Properties Measurements. Following our customary procedure of providing some characterization of metallic/semiconduction properties of such phases,³ electrical resistivities were measured by the electrodeless "Q" method with the aid of a Hewlett-Packard 4342A Q meter.²¹ The method is particularly suitable for measurements on highly air-sensitive samples. For this purpose, 68.9, 98.6, and 102 mg of powdered I, II, and III, respectively, with grain diameters between 150 and 250 μm were dispersed with chromatographic alumina and sealed in Pyrex tubes. Measurements were made at 34 MHz over the range 80–260 K. All three measured resistivities increase linearly over the temperature range, this change being taken as the defining characteristic of a metallic substance, but with different mean temperature dependencies. The extrapolated ρ₂₉₈ values are about 45.8, 90.9, and 162 μΩ·cm for I, II, and III, respectively. Magnetic susceptibility data for II were obtained from a 65.5 mg ground powder sealed under He in the container type described elsewhere.²² The magnetization was measured over the range 6–330 K on a Quantum Design MPMS SQUID magnetometer. The results were positive and almost temperature-independent, (1.08–1.13) × 10⁻³ emu/mol over 25–330 K, after correction for the container, ion cores, and Larmor precession of the valence electron pairs in the large orbitals of each cluster.²³ Graphical data for these electrical resistivities and magnetic susceptibilities are in the Supporting Information.

Band Structure Calculations. Electronic structure tight binding calculations were performed using the extended Hückel method and the CAESAR program package developed by Whangbo and co-workers,²⁴ in each case for the observed valence electron content of the phase. Calculations were first performed on the ideal In₁₀₅³⁴⁻ anionic network of compound I but with 100% indium site occupancies. Calculations for the Li example I were done with all atom positions necessary to describe the structure in P1 so that different isolated Li atoms could be input that gave close to the observed stoichiometry. The choices had no effect on the results. The following indium and lithium atomic orbital energies and exponents were employed for the calculations (*H_{ii}* = orbital energy, eV; *ξ* = Slater exponent): 5s –12.6, 1.903; 5p –6.19, 1.677 and 2s –5.4, 0.65; 2p –3.5, 0.65, respectively.²⁵

(21) Zhao, J. T.; Corbett, J. D. *Inorg. Chem.* **1995**, *34*, 378.

(22) Sevov, S. C.; Corbett, J. D. *Inorg. Chem.* **1991**, *30*, 4875.

(23) Selwood, P. W. *Magnetochemistry*, 2nd ed.; Interscience Publishers: New York, 1956; p 70. Ashcroft, N. W.; Mermin, D. N. *Solid State Physics*; Holt, Rinehart and Winston: Philadelphia, PA, 1976; p 649.

(24) Ren, J.; Liang, W.; Whangbo, M.-H. *CAESAR for Windows*, Prime-Color Software, Inc.: North Carolina State University: Raleigh, NC, 1998.

(25) Canadell, E.; Eisenstein, O.; Rubio, J. *Organometallics* **1984**, *3*, 759.

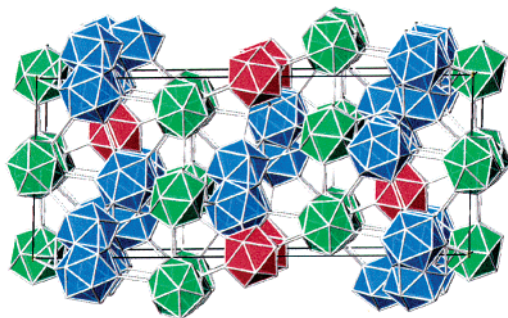


Figure 1. $\sim[100]$ view of the unit cell of $\text{K}_{14}\text{Na}_{20}\text{In}_{91.818(8)}\text{Li}_{13.182(8)}$ (**II**) with the different cluster types: icosahedra A (green), B (red), and triply fused icosahedra in In_{28} C (blue). K and Na atoms are omitted for clarity. The c -axis is horizontal.

Results and Discussion

Crystal Structures. The three isotopic- $\text{K}_{34}\text{In}_{92.30}\text{Li}_{12.70}$ (**I**), $\text{K}_{14}\text{Na}_{20}\text{In}_{91.82}\text{Li}_{13.18}$ (**II**), and $\text{K}_{14}\text{Na}_{20}\text{In}_{96.30}$ (**III**) (all $R\bar{3}m$) phases contain very similar three-dimensional indium networks composed of different building blocks: two types of icosahedra (A and B) and In_{28} from triply fused icosahedra (C). The general view of the unit cell of compound **II** in Figure 1 outlines the three-dimensional indium network in which all In–In separations less than 3.5 Å are marked. Icosahedra A (green) and B (red) are centered at Wyckoff sites $9e$ and $3b$ with $2/m$ and $\bar{3}m$ symmetries, respectively. Both icosahedra are exo-bonded at all vertices via direct intercluster In–In bonds to the same or other clusters, as shown Figure 2a and b. Sites of partial Li substitution are in black. Twenty ordered alkali metal atoms (Na (yellow) or K (orange)) surmount the triangular faces of all icosahedra to generate the dual pentagonal dodecahedra, and these also serve to bridge between clusters. The In_{28} polyhedron (blue, Figure 2c) results from condensation of three icosahedra, each sharing a face with two neighbors. One atom (In14, on the 3-fold axis) is common to all three icosahedra. This In_{28} polyhedron is surmounted by 28 alkali metals. Two of the triply fused icosahedra (In_{28} polyhedra) further aggregate to give the sandwich complex (In_{28}) $\text{In}(\text{In}_{28})$ via a six-coordinate interbridging In15 atom that caps a trigonal face of each In_{28} , Figure 3a. Such triply fused icosahedra have been encountered before in β -rhombohedral boron as well as in the structurally very similar phases $\text{Na}_{13}\text{K}_4\text{Ga}_{49.57}$ ⁸ and $\text{Na}_{34}(\text{MGA})_{105}$ ($M = \text{Cu}, \text{Zn}$) (for which mixed sites were not resolved).⁹ The latter also has sandwich complexes. Compound **I** has the same structure as compound **II** except that all 20 Na atoms have been replaced by K.

Compound **III**, without lithium, shows basically the same structure as compounds **I** and **II**, but pairs of bridging In15 at Wyckoff site $6c$ mean that two triply fused In_{28} polyhedra are further interconnected by an In15–In15 pair bond (2.673 Å), as shown in Figure 3b. However, it should also be noted that these and some adjoining In atoms in **III**-C have fractional occupancies (blue spheres), and these evidently result in the 2-fold disorder of In11 and In14 as well. Other examples include disordered Ni@In₁₀ clusters inside fullerene-like In₆₀ and In₇₄ cages in $\text{Na}_{96}\text{In}_{\sim 97}\text{Ni}_2$ and $\text{Na}_{\sim 172}\text{In}_{\sim 197}\text{Ni}_2$ ²⁶ and the disordered *arachno*-Sn₈ cluster that evidently resides inside a Na₂₂ cage

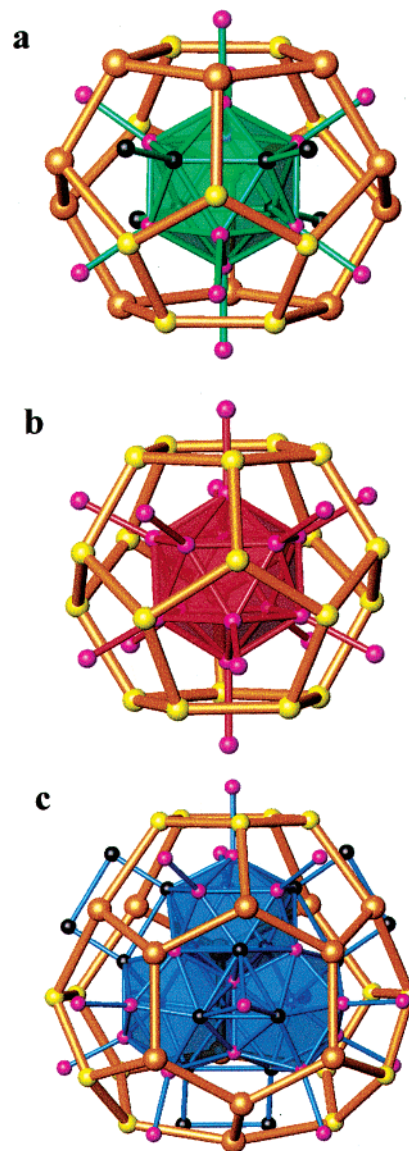


Figure 2. Building units in $\text{K}_{14}\text{Na}_{20}\text{In}_{91.818(8)}\text{Li}_{13.182(8)}$ (**II**): (a) icosahedron A surrounded by 20 cations (10K (orange) + 10Na (yellow)); (b) icosahedron B surrounded by 20 Na cations; (c) In_{28} unit C surrounded by 28 cations (15Na + 13K), which is formed by face-sharing of three icosahedra. The exo atoms in all views are vertices in other clusters. Sites of partial Li substitution are black.

in $\text{Ba}_{16}\text{Na}_{204}\text{Sn}_{310}$.²⁷ The disorder in compound **III** is presumably related to the fractional occupancies of the neighboring atoms. As explained by Bobev and Sevov,²⁷ split positions are generated according to whether the neighboring site is occupied or empty. The disorder disappears in compounds **I** and **II** in which there is full (sometimes mixed) occupancy of all positions. The stability of the defect-free (In_{28}) $\text{In}(\text{In}_{28})$ complex also appears to be increased by relaxation of the polyhedral framework through enlargement of the triangle that is capped by interconnecting In15, Figure 3.

As mentioned before, the cations around the In_{12} and In_{28} building blocks generate the respective A_{20} and A_{28} cages ($A = \text{Na}, \text{K}$) in a ratio of 2:1 and these in turn form an A_{136} clathrate-II type network.²⁸ This arrangement around different sized anionic clusters has already been found in many

(26) Sevov, S. C.; Corbett, J. D. *Science* **1993**, *202*, 880. Sevov, S. C.; Corbett, J. D. *J. Solid State Chem.* **1996**, *123*, 344.

(27) Bobev, S.; Sevov, S. C. *J. Am. Chem. Soc.* **2001**, *124*, 3359.

(28) Claussen, W. F. *J. Chem. Phys.* **1951**, *19*, 1425.

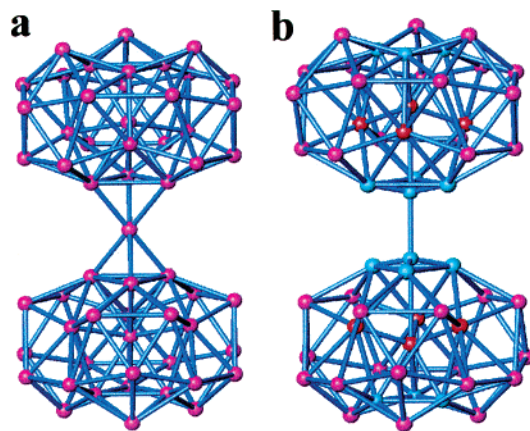


Figure 3. (a) Sandwich complex of two triply fused icosahedra bridged by a six-coordinate In_{15} atom in compounds **I** and **II**; (b) two triply fused In_{28} polyhedra interconnected by In–In dimer in compound **III**. (Blue atoms have fractional occupancies; red atoms mark the centers of the split positions in the last.)

other compounds, e.g., $\text{K}_{17}\text{In}_{41}$, $\text{K}_{39}\text{In}_{80}$, $\text{K}_{22}\text{In}_{39}$, $\text{Na}_{22}\text{Ga}_{39}$, $\text{Na}_{35}\text{Cd}_{24}\text{Ga}_{56}$, $\text{K}_{21-\delta}\text{Na}_{2+\delta}\text{In}_{39}$ ($\delta = 2.8$), and $\text{Na}_{12}\text{K}_{18}\text{In}_{53}\text{Tl}_7$.^{29,30} The presence of this regular cation array is probably decisive in the formation of these structures; the special cation arrangement not only fills space more efficiently but also keeps the clusters apart. Further condensation or interbridging of poly-anions would presumably result were they to come in contact.

Mixing of Indium and Lithium. Compounds between alkali metals Na–Cs and group 13 elements generally exhibit a reduction of the latter, more electronegative elements by the active elements, which then fulfill typical cation roles. In terms of the Mulliken electronegativity scale³¹ for neutral atoms, lithium is the least electropositive species among all alkali metals (Li, 3.01; Na, 2.85; K, 2.42) and its electronegativity is in fact close to that of indium (3.1). Thus, the preferred electron donor in these K–(Na)–Li–In systems is K (Na), and Li instead mixes with In at the least negative cluster sites. Of course, lithium is significantly different from its heavier homologues in its physical and chemical properties. A higher electron affinity and stronger polarizing power allow lithium to assume the largest amount of covalent bonding throughout this series.²⁰ In particular, many Li phases show close contacts of these with anionic network atoms from group 13 or 14 atoms that may be rationalized using Zintl–Klemm viewpoints. Several compounds are known with substructure networks of mixed Li and Al atoms, for instance, in a series of $\text{CaLi}_x\text{Al}_{2-x}$ compounds in various Laves phase structures in which mixed atoms form 3636 nets.³² Three related structures in $\text{Ca}_6\text{Li}_x\text{Al}_{23-x}$, $\text{Sr}_9\text{Li}_{7+x}\text{Al}_{36-x}$, and $\text{Ba}_2\text{Li}_{3+x}\text{Al}_{6-x}$ have the same basic clusters, tetrahedral stars, and double tetrahedral stars.³³ The nonexistence of any corresponding binary K–In cluster compound in the present work without either lithium substitution (**I**) or the formation of appreciable indium defects (**III**) indicates that only lattices electron-poorer than the ideal $\text{A}_{34}\text{In}_{105}$ ($\text{A} = \text{K}$ or Na) are stable and that lithium (or perhaps other small low-valent atoms) is evidently necessary to gain an ordered structure. An intimate

relationship between the crystal structure and its valence electron requirements is clear.

Electronic Structure and Chemical Bonding. Simply counting the electrons needed for bonding in the different segments of many structures of valence (Zintl) phases has often proven to be a very useful, even elegant, method for rationalizing the bonding.^{2,3,34} But skeletal electron counts are difficult to ascertain or forecast for intricate structures, particularly those in which partial occupancies occur. Fortunately, compounds **I** and **II** appear to be substantially defect-free, with all crystallographic sites fully occupied. For complex clusters, counting schemes such as those of Wade³⁵ no longer work. The rules developed by Mingos³⁶ as well as by Teo³⁷ for polyhedral condensation work well for fusion of transition metal clusters but sometimes give unsatisfactory results for main-group elements, and they are difficult to apply to some condensed polyhedra. Recently, Jemmis et al.³⁸ have extended Wade's rules to explain the electronic requirements of condensed polyhedral boranes in terms of an *mno* rule in which $m + n + o$ electron pairs are necessary for a multipolyhedral borane system to be stable, with m as the number of polyhedra, n as the number of vertexes, and o as the number of single-vertex-sharing connections. The applicability of the *mno* rule has been demonstrated for a variety multipolyhedral boranes and heteroboranes, but, up to now, only for boranes. Since Ga, In, and Tl are congeners of B, we have tried to apply this rule to known heavier triel polyhedra. (Of course, Wade's treatment is a special case of the *mno* rule ($m = 1$, $o = 0$), and these fits represent nothing new.) We find that the Jemmis version also works for 18b-Ga_{11} in $\text{Li}_9\text{K}_3\text{Ga}_{28,8}$,⁴⁰ ($\text{Ga}_{11}\text{LiGa}_{11}$) in Li_5Ga_9 ,⁴¹ and (Ga,Zn)₂₉ in $\sim\text{Li}_{38}\text{Zn}_{34,0}\text{Ga}_{66,9}$.⁴²

In the present structures, the $(\text{In}_{28})\text{In}(\text{In}_{28})$ association is predicted to require $m + n + o = 8 + 57 + 1 = 66$ skeletal electron pairs or 132 electrons for stability. To this must be added exo bond requirements. Ten In that are shared in the triply fused In_{28} polyhedron and the single atom interconnecting two In_{28} have no further bonding, whereas the other $57 - 21 = 36$ atoms are exo-bonded to other clusters. Thus 36 more electrons and a total of 168 are required for the In_{57}^{3+} cluster, which also corresponds to that cited for $\text{B}_{57}\text{H}_{36}$.⁴² Of course, the former is not known alone or in the presence of four interbridging In_{12}^{-2} in **III**, rather only as a defect In_{58} unit, approximately $(\text{In}_{48,3}\text{V}_{9,7})^{-26}$ ($\text{V} = \text{vacancy}$) according to the stoichiometry of **III** and a presumed normal behavior of the four separable In_{12} clusters (see below for qualifications). The extra electrons therein can be viewed as lone pairs more or less localized around vacancies. When the electron count in icosahedron **A** is reduced by Li substitution, the fused cluster **C** transforms to the

(29) Carrillo-Cabrera, W.; Caroca-Canales, N.; von Schnering, H.-G. *Z. Anorg. Allg. Chem.* **1994**, *620*, 247.

(30) Li, B.; Corbett, J. D. *Inorg. Chem.* **2003**, *42*, 8768.

(31) Pearson, R. G. *Inorg. Chem.* **1988**, *27*, 734.

(32) Nesper, R.; Miller, G. J. *J. Alloys Compd.* **1993**, *197*, 109.

(33) Haussermann, U.; Worle, M.; Nesper, R. *J. Am. Chem. Soc.* **1996**, *118*, 11789.

(34) Eisenmann, B.; Cordier, G. In *Chemistry, Structure and Bonding of Zintl Phases and Ions*; Kauzlarich S., Ed.; VCH Publishers: New York, 1996; Chapter 2.

(35) Wade, K. *Chem. Commun.* **1971**, 792.

(36) Mingos, D. M. P. *Chem. Commun.* **1983**, 706. Mingos, D. M. P. *Acc. Chem. Res.* **1984**, *17*, 311.

(37) Teo, B. K. *Inorg. Chem.* **1984**, *23*, 1251. Teo, B. K. *Inorg. Chem.* **1985**, *24*, 4209.

(38) Balkarishnarajan, M. M.; Jemmis, E. D. *J. Am. Chem. Soc.* **2000**, *122*, 456. Jemmis, E. D.; Balkarishnarajan, M. M.; Pancharatna, P. D. *J. Am. Chem. Soc.* **2001**, *123*, 4313. Jemmis, E. D.; Balkarishnarajan, M. M.; Pancharatna, P. D. *Chem. Rev.* **2002**, *102*, 93.

(39) Belin, C. *J. Solid State Chem.* **1983**, *50*, 225.

(40) Charbonnel, M.; Marteghetti, A.; Belin, C. *Inorg. Chem.* **2000**, *39*, 1684.

(41) Tillard-Charbonnel, M.; Chouaibi, N.; Belin, C.; Lapasset, J. *Eur. J. Sol. State Inorg. Chem.* **1992**, *29*, 347.

(42) Jemmis, E. D.; Balkarishnarajan, M. M. *J. Am. Chem. Soc.* **2001**, *123*, 4324.

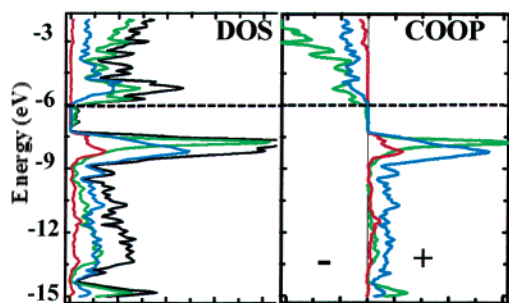


Figure 4. (Left) Densities-of-states (DOS) data for ideal indium framework In_{105}^{-34} . The total DOS is black, and the projected partial DOS contributions of indium within icosahedra A, B and the sandwich complex (C) are green, red, and blue, respectively. (Right) COOP curves for In–In bonds within icosahedron A, B and the triply fused In_{28} icosahedra are colored green, red, and blue, respectively. The dashed lines denote the Fermi energy corresponding to 969.4 valence electrons, the experimental average determined for **I** and **II**.

stoichiometric ($\sim\text{In}_{47.6}\text{Li}_{9.34}$)^{-15.7} by, principally, Li addition and oxidation. In the refined structures of **I** and **II** ($Z = 3$), there are nine 12-bonded ($\text{In}_{10.9}\text{Li}_{1.1}$) A, three 12-bonded In_{12} B, and three stoichiometric 36-bonded ($\text{In}_{47.6}\text{Li}_{9.4}$) C in the unit cell. Utilizing Wade’s $2n + 2$ electron pair rules for the icosahedra, plus a one electron contribution for each exo bond, the total electrons required are $9(26 + 12) + 3(26 + 12) + 3(132 + 36) = 960$. The polyhedral requirements are presumed to not be altered by Li substitution, only the number of electrons available.

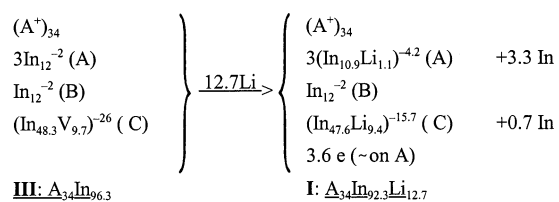
To have a more detailed understanding of the chemical bonding and the preferences for substitution or vacancies in the clusters, extended Hückel band calculations have been performed on (a) the complete ideal indium framework In_{105}^{-34} ($Z = 3$) and (b) the Li product $\text{In}_{92.3}\text{Li}_{12.7}^{-34}$ with the parameters of **I** and the experimental electron populations. According to the Zintl–Klemm concept, it is assumed that the alkali metals donate their electrons to the anionic lattice of the more electronegative elements, and these nuclei were not (and cannot be well) included in EHTB calculations. Figure 4 illustrates the densities-of-states (DOS) and crystal orbital overlap population (COOP) curves for the anionic lattice in **I**. DOS curves show the total (black) and three partial projections for indium s plus p orbital contributions within icosahedra A (green), B (red), and in sandwich complex C (blue), respectively, and the COOP curves show the relevant In–In interactions within those three units. There is a distinct minimum in DOS starting at ~ -7.34 eV which corresponds to the 960 valence electrons per cell that was deduced according to the foregoing empiricisms. The average observed electron count per cell for **I** (970.79(4)) and **II** (967.91(5)) is 969.4, which places the observed Fermi energy at -6.02 eV (dotted line), cutting through a very low DOS consisting mainly of states on the In_{12} icosahedron A. The calculated electron count of 960 is 99% of those present according to refined compositions, a remarkable closure that is probably within total uncertainties, since only semiquantitative results might be expected from the extended Hückel approach. In the intervening pseudogap, about three electrons per f.u. are bound in a low densities-of-states region, principally on cluster A in largely nonbonding states that turn weakly antibonding on approach to the experimental E_F . These compounds are, in accord with the behavior of a great number of other triel phases,³ all poorly metallic according to both resistivity and magnetic

susceptibility measurements (Supporting Information), and so the highest states cannot be all localized. Compound **II** also appears to be substantially stoichiometric; provision of additional Li values in another syntheses reaction did not appear to lower the In fractions and thence E_F . This suggests that some local site energies may be tilted in favor of In, particularly in A.

On the other hand, generally, the electron count of the hypothetical defect-free $\text{A}_{34}\text{In}_{105}$, $1047 e^-$, would place E_F at -5.25 eV, within strongly antibonding states on both icosahedron A and sandwich complex C. This improbability is solved either by mixing the electron-poorer Li with indium in clusters A and C in **I** and **II** or, lacking this option, by the formation of fractional In occupancies in complex C in **III**. Two other isostructural compounds, $\text{K}_{34}(\text{M},\text{In})_{105}$ ($\text{M} = \text{Mg}$ and Zn) in which there are electronically comparable substitutions of Mg and Zn for some In, further demonstrate these general relationships between the structure and electronic requirements.⁴³

As expected from band calculations for $\text{K}_{34}\text{In}_{105}$, defects in the indium network are preferentially located at the particularly “unstable” (In_{28}) $\text{In}(\text{In}_{28})$ cluster. Mulliken atom population calculations for the ideal all-In phase show that the appropriate 4 of the 15 crystallographic sites have the lowest populations: In_2 , 3.03; In_4 , 2.98; In_{12} , 2.96; and In_{13} , 2.94, with those for all others sites falling between 3.07 and 3.75. In both **I** and **II**, substitutions of lithium for some indium occur at just these four sites, by which the ideal polyhedron electron count for C (168) is lowered to 152.3 electrons. Alternatively, energetic stabilization can be achieved by the formation of vacancies in C in $\text{K}_{14}\text{Na}_{20}\text{In}_{96.30(1)}$ (**III**). Although the defects and disorder make it difficult to determine the required number of electrons in this polyhedron, a decrease is evident. Importantly, there are 968.7 valence electrons in **III** as refined, quite close to the average in **I** and **II** (969.4) and also to that calculated in the ideal model.

The scheme below is intended to give a clearer appreciation of the redox reactions that occur when Li is added to the defect-laden **III** (per formula unit). The approximate cluster charges follow the assumed homolytic cleavage of all intercluster bonds, which is of course overstated for a metallic phase. Assuming



neutral atoms for the Li added and In removed, each A cluster is reduced by 2.2 e, whereas insertion of Li into C (the defect 58 vertex cluster) results in a $10.3 e^-$ oxidation (and a 57-atom cluster). A small $3.6 e^-$ residual per formula unit reflects the higher E_F observed for **I** and **II** than expected from the ideal model if that is assumed to be precise. Although the process is not as simple as portrayed above, the internal redox and substitution processes that differentiate **I** and **II** from **III** (In only) in a nearly fixed lattice are rather remarkable.

Conclusions

Structural stabilization among these three compounds reveals an intimate relationship between structure and valence electron

(43) Li, B.; Corbett, J. D. Unpublished results.

requirements. In these unusual examples, electronic tuning within the complicated network structure is realized either by substitution of part of the indium by electron-poorer lithium atoms or by introduction of occupancy defects (and disorder) along with structural perturbations. A special role of lithium is shown in compounds **I** and **II** by its mixture into the indium anionic clusters. More such compounds are expected to arise whenever we introduce lithium into other active metal indium compounds. However, it is still possible that more electron-neutral and stoichiometric phases will instead accommodate lithium cations in suitable cavities among the polyanions. Considerations of the mixed In/Li clusters are continuing.

Acknowledgment. We are indebted to S. Budko for the magnetic susceptibility data. This article is dedicated to Professor Arndt Simon on the occasion of his 65th birthday.

Supporting Information Available: Additional crystallographic and refinement parameters for all three compounds in cif format; electron density maps and figures of the atom numbering in the clusters, resistivity and susceptibility data, and band calculation results for the mixed In–Li network. This material is available free of charge via the Internet at <http://pubs.acs.org>.

JA0402046